

## **Muscarinic receptors as model targets and antitargets for structure-based ligand discovery**

Andrew C. Kruse, Dahlia R. Weiss, Mario Rossi, Jianxin Hu, Kelly Hu, Katrin Eitel, Peter  
Gmeiner, Jürgen Wess, Brian K. Kobilka & Brian K. Shoichet

Department of Molecular and Cellular Physiology, Stanford University School of Medicine,  
Stanford, California (A.C.K., B.K.K.), Department of Pharmaceutical Chemistry, University of  
California, San Francisco, California (D.R.W., B.K.S.), Faculty of Pharmacy, University of  
Toronto (B.K.S.), Molecular Signaling Section, Laboratory of Bioorganic Chemistry, National  
Institute of Diabetes and Digestive and Kidney Diseases, Bethesda, Maryland (M.R., J.H., K.H.,  
J.W.), Department of Chemistry and Pharmacy, Friedrich Alexander University, Erlangen,  
Germany (K.E., P.G.).

Running Title: Structure-based ligand discovery for muscarinic receptors

Corresponding authors:

Brian Kobilka, Molecular and Cellular Physiology and Medicine, Stanford University,  
157 Beckman Center, 279 Campus Drive, Stanford, CA 94305-5345

Telephone: (650) 723-7069; Fax: (650) 498-5092; Email: [kobilka@stanford.edu](mailto:kobilka@stanford.edu)

Brian Shoichet, Faculty of Pharmacy, Donnelly Centre, University of Toronto, 160 College St.,  
Toronto, ON Canada, M5S 3E1. Telephone: (416) 978-7224; Email: [bshoichet@gmail.com](mailto:bshoichet@gmail.com)

**# of text pages**            **30**

**# of tables**            **2**

**# of figures**            **4**

**# of references**            **42**

**# of words in the Abstract**    **239**

**# of words Introduction**        **416**

**# of words Discussion**            **923**

**Abbreviations:** GPCR: G protein-coupled receptors; NMS: N-methyl scopolamine; OXO-M: oxotremorine-M; QNB: quinuclidinyl benzilate; cAMP: cyclic AMP; LE: Ligand efficiency;  $T_c$ : Tanimoto coefficient;

## Abstract

G protein-coupled receptors (GPCRs) regulate virtually all aspects of human physiology and represent an important class of therapeutic drug targets. Many GPCR-targeted drugs resemble endogenous agonists, often resulting in poor selectivity among receptor subtypes and restricted pharmacological profiles. The muscarinic acetylcholine receptor family exemplifies these problems; thousands of ligands are known, but few are receptor subtype-selective and almost all are cationic in nature. Using structure-based docking against the  $M_2$  and  $M_3$  muscarinic receptors, we screened 3.1 million molecules for ligands with new physical properties, chemotypes, and receptor subtype-selectivities. Of 19 docking-prioritized molecules tested against the  $M_2$  subtype, 11 had substantial activity and 8 represented new chemotypes. Intriguingly, two were uncharged ligands with low micromolar to high nanomolar  $K_i$  values, an observation with few precedents among aminergic GPCRs. To exploit a single amino-acid substitution among the binding pockets between the  $M_2$  and  $M_3$  receptors, we selected molecules predicted by docking to bind to the  $M_3$  and but not the  $M_2$  receptor. Of 16 molecules tested, eight bound to the  $M_3$  receptor. Whereas selectivity remained modest for most of these, one was a partial agonist at the  $M_3$  receptor without measurable  $M_2$  agonism. Consistent with this activity, this compound stimulated insulin release from a mouse b-cell line. These results support the ability of structure-based discovery to identify new ligands with unexplored chemotypes and physical properties, leading to new biological functions, even in an area as heavily explored as muscarinic pharmacology.

## Introduction

G protein-coupled receptors (GPCRs) are integral transmembrane proteins that transduce extracellular signals from neurotransmitters, hormones, odorants, and many other signals across cellular membranes. The muscarinic acetylcholine receptors (M<sub>1</sub>-M<sub>5</sub>) are a subfamily of GPCRs recognizing the neurotransmitter acetylcholine and signaling through G proteins of the G<sub>q/11</sub> class (M<sub>1</sub>, M<sub>3</sub>, and M<sub>5</sub> subtypes), and the G<sub>i/o</sub> class (M<sub>2</sub> and M<sub>4</sub> subtypes). These receptors are targets for the treatment of many illnesses, including chronic obstructive pulmonary disease, urinary incontinence, and diabetes (Wess et al., 2007), and have been implicated in treatment of cognitive disorders such as Alzheimer's disease (Messer, 2002), and schizophrenia (Chan et al., 2008).

Tool and drug development at muscarinic receptors has been complicated by difficulties in finding subtype-selective ligands. None of the muscarinic agonists and antagonists currently used in the clinic are selective for a particular muscarinic receptor subtype. This reflects the high sequence identities among the orthosteric sites of the M<sub>1</sub>-M<sub>5</sub> receptors, differing, for instance, between the M<sub>2</sub> and M<sub>3</sub> subtypes by only a single residue. Muscarinic receptors can also mediate various side effects (e.g., adverse effects on heart rate, salivary secretion, and smooth muscle contractility). For instance, whereas recent evidence suggests that an M<sub>3</sub> agonist would promote insulin release in type 2 diabetes (Wess et al., 2007), M<sub>2</sub> agonism would have substantial cardiac effects that would complicate clinical use. Similarly, M<sub>1</sub> agonists have shown promise for treatment of Alzheimer's disease, but dose-limiting side effects have precluded clinical use (Caccamo et al., 2009). Consequently, recent attempts to develop selective muscarinic drugs have focused on ligands targeting either an allosteric site (Conn et al., 2009b), or both orthosteric and allosteric sites simultaneously (Mohr et al., 2010).

The recent determination of the crystal structures for the M<sub>2</sub> and M<sub>3</sub> muscarinic receptor subtypes (Haga et al., 2012b; Kruse et al., 2012) enables a structure-based discovery program for novel muscarinic ligands. To discover new chemotypes and compounds with novel physical and pharmacological properties, we initially docked large compound libraries against the M<sub>2</sub> muscarinic structure. A high discovery rate of new chemotypes and new physical properties inspired us to seek M<sub>3</sub>-selective molecules by exploiting the small region of sequence difference between the two receptor subtypes. Whereas most molecules displayed some selectivity for the M<sub>3</sub> subtype, as designed in the docking screen, this selectivity was modest, illustrating the challenges of discovering subtype-selective orthosteric muscarinic ligands. However, the discovery of a partial M<sub>3</sub> agonist that had no agonist activity at the M<sub>2</sub> receptor, and its efficacy in a cell-based model to promote insulin release in  $\beta$ -cells, also illustrates the potential of this approach.

## Materials and Methods

### *Materials.*

Compounds were obtained from the vendors Molport, Chembridge, Enamine, Scientific Exchange, Princeton Biomolecular Research and Asinex, as well as from the Developmental Therapeutics Program at the National Cancer Institute. All compounds were sourced at 95% or greater purity as described by the vendors. All active compounds were further tested for purity by LC/MS at UCSF, and were found to be at least 95% pure as judged by peak height and identity. For compounds 11 and 12, LC/MS was inconclusive and purity was confirmed by <sup>1</sup>H NMR spectroscopy at the Stanford Magnetic Resonance Laboratory using a Varian Inova 600 MHz spectrometer. Compound 5 was not commercially available in sufficient purity, and details regarding its preparation are given below.

### **Chemistry.**

Compound 5 (pyridin-3-ylmethyl 2-hydroxy-2,2-diphenylacetate) was not commercially available in sufficient purity, and was synthesized as follows. After stirring a suspension of 3-(hydroxymethyl)pyridine (30  $\mu$ L, 0.31 mmol) and  $K_2CO_3$  (100 mg, 0.72 mmol) in anhydrous DMF (12 mL) at room temperature for 1 h, a solution of methyl benzilate (50 mg, 0.21 mmol) in anhydrous DMF (3 mL) was added. The mixture was stirred at 65  $^{\circ}C$  at 70-100 mbar for 6 h and allowed to cool to room temperature. After addition of  $CH_2Cl_2$  and water, the organic layer was washed with a saturated aqueous solution of NaCl, dried ( $Na_2SO_4$ ) and evaporated. The residue was purified by flash chromatography ( $CH_2Cl_2$  – MeOH 60:1) to yield pure pyridin-3-ylmethyl 2-hydroxy-2,2-diphenylacetate (24.3 mg, 36 %) as a white solid (mp: 98-101  $^{\circ}C$ ).  $^1H$  NMR ( $CDCl_3$ , 600 MHz)  $\delta$  from TMS (ppm): 8.58 (brs, 1H), 8.51 (brs, 1H), 7.52 (brd, J = 7.6 Hz, 1H), 7.37-7.41 (m, 4H), 7.30-7.34 (m, 6H), 7.26-7.27 (m, 1H), 5.31 (s, 2H), 4.15 (brs, 1H);  $^{13}C$  NMR ( $CDCl_3$ , 150 MHz)  $\delta$  from TMS (ppm): 174.3, 149.3, 148.8, 141.7, 136.6, 131.1, 128.4, 128.3, 127.5, 123.9, 81.4, 65.7; IR (NaCl),  $\nu$  ( $cm^{-1}$ ): 3150, 3060, 1740, 1600, 1580, 1450, 1220, 1060, 700; HPLC:  $t_R$  = 18.55 min (eluent 1),  $t_R$  = 16.41 min (eluent 2), purity > 95 %; HRMS ( $m/z$ ):  $[M]^+$  calcd for  $C_{20}H_{17}NO_3$  (M +  $Na^+$ ) 342.1101, found 342.1111.

IR spectra were recorded on a JASCO model FTIR 410 instrument as a film on NaCl.  $^1H$  NMR (600 MHz) and  $^{13}C$  NMR (150 MHz) spectra were determined on a Bruker AVANCE 600 spectrometer. ESI-ToF high mass accuracy and resolution experiments were performed on a Bruker maXis MS in the laboratory of the Chair of Bioinorganic Chemistry, FAU. HPLC analysis was performed on an analytical system (Agilent 1100 analytical series, VWD detector, Zorbax Eclipse XDB-C8 analytical column, 4.6 $\times$ 150 mm, 5  $\mu$ m, flow rate: 0.5 ml/min). Eluent 1:  $CH_3OH$  in  $H_2O$  + 0.1%  $HCO_2H$  (0-3 min 10 %, 3-18 min 10 – 100%, 18-24 min 100%); eluent 2:  $CH_3CN$  in  $H_2O$  + 0.1%  $HCO_2H$  (0-3 min 5 %, 3-18 min 5-85%, 18-24 min 85%). Flash chromatography

was done using silica gel (40-63  $\mu\text{m}$ ) as stationary phase. The purity of the test compound was determined to be >95%.

### ***Molecular docking.***

To predict new muscarinic ligands, we used DOCK 3.6 (Lorber and Shoichet, 2005; Irwin et al., 2009; Mysinger and Shoichet, 2010) to virtually screen the approximately 3.1 million lead-like and fragment-like subsets of ZINC (Irwin and Shoichet, 2005; Irwin et al., 2012) against the  $M_2$  or  $M_3$  muscarinic receptor structure. Compounds were docked in multiple orientations and multiple conformations. Each geometry was scored for electrostatic and van der Waals complementarity, and corrected for desolvation using the solvent-excluded volume method, and the complex with the lowest energy was picked. Compounds were manually selected for experimental testing from the top-ranking 500 molecules based both on their physical complementarity and chemical novelty, using criteria previously described (Mysinger et al., 2012).

To identify compounds that selectively bind to the  $M_3$  receptor, a similar method was first employed to score lead-like and fragment-like subsets of ZINC against both receptors. The top 5,000 ranked molecules against the  $M_3$  receptor were selected for further consideration. Each of these molecules was then ranked according to the difference in energy score between docking at  $M_3$  and  $M_2$ . The 500 molecules with the largest energy score difference in favor of the  $M_3$  receptor were then inspected and 16 were chosen for experimental testing on the basis of high physical and chemical complementarity to  $M_3$ , poor complementarity to  $M_2$ , and novelty.

### ***Receptor expression and membrane preparation.***

Human  $M_2$  and rat  $M_3$  muscarinic receptors were expressed with an amino-terminal FLAG epitope tag in Sf9 insect cells using the BestBac system (Expression Systems). Membranes

were prepared using a glass dounce tissue grinder to homogenize cells in 20 mM Tris pH 7.5 and 1 mM EDTA. Homogenized cell material was then centrifuged at low speed (100 × G) for 5 min to remove debris. The supernatant was then centrifuged at 18,000 rpm in an SA-800 rotor for 15 min to pellet membranes. Membranes were resuspended in binding buffer (75 mM Tris, pH 7.4, 12.5 mM MgCl<sub>2</sub>, 1 mM EDTA), aliquoted, and flash frozen in liquid nitrogen.

### ***Radioligand binding assays.***

Ligand affinities were measured by radioligand displacement binding assays. Binding assays were performed using <sup>3</sup>H-N-methyl scopolamine (NMS; Perkin Elmer) at 0.61 nM in all samples. Following mixing of membranes, cold ligand and NMS samples were shaken at 20 °C for two hours. Samples were then filtered on a glass fiber filter with a 48-well harvester (Brandel). Radioactivity was measured by liquid scintillation. Binding data are summarized in Tables 1 and 2, and representative binding curves are shown in figures S1, S2, and S3. Binding data analysis was performed using GraphPad Prism 4.0 software.

### ***Calcium Mobilization Assay.***

CHO cells stably expressing the human M<sub>3</sub> receptor or CHO cells stably co-expressing the human M<sub>2</sub> receptor and a hybrid G protein G<sub>qi</sub>5 (Marlo et al., 2009) (a G<sub>aq</sub> subunit in which the last five amino acids were replaced with the corresponding G<sub>ai</sub> sequence) were incubated with increasing concentrations of ligands, and changes in intracellular calcium levels were determined using FLIPR technology (Molecular Devices, Sunnyvale, CA). All measurements were performed in 96-well plates, as described previously (Li et al., 2007; McMillin et al., 2011). Agonist concentration-response curves were analyzed using GraphPad Prism 4.0 software.

### ***cAMP Assay.***



CHO cells stably expressing the human M<sub>2</sub> receptor were trypsinized, collected by centrifugation, and resuspended in phosphate-buffered saline containing glucose (1 mg/ml) and EDTA-free complete protease inhibitor (Roche Applied Science) at a density of 1 × 10<sup>6</sup> cells/ml. Subsequently, 20 µl aliquots were added to 200 µl PCR tubes and incubated with the same volume (20 µl) of increasing concentrations of ligands in the presence of 50 µM forskolin for 25 min at 37°C. The incubation mixtures were then transferred into white-bottom 384-well plates (□5000 cells/well), and cells were lysed to determine drug-dependent changes in cAMP levels using a fluorescence resonance energy transfer-based cAMP detection technique (cAMP dynamic 2 kit; Cisbio Bioassays, Bedford, MA) according to the manufacturer's protocol. Elevated 665 nm/620 nm ratio indicates decreased cAMP levels in this assay.

#### ***Insulin release assays (MIN6 cells).***

MIN6 cells (a kind gift from Dr. Abner Notkins, NIDCR, NIH) were cultured as described previously (Ishihara et al., 1993). 60,000 cells were seeded into 96 well plates and cultured for 48 hr at 37 °C in 5% CO<sub>2</sub>. After this time, MIN6 cells were washed with 3.3 mM glucose buffer (in Krebs-Ringer bicarbonate/HEPES buffer) and then incubated for 1 hr at 37 °C in 5% CO<sub>2</sub>. After this step, MIN6 cells were incubated for another hour at 37 °C in 5% CO<sub>2</sub> with increasing concentrations of oxotremorine-M (OXO-M) or compound 16 in 16.7 mM glucose Krebs-Ringer buffer. Insulin release was determined by measuring insulin concentrations in the incubation medium using an insulin ELISA kit (Crystal Chem Inc., Downers Grove, IL, USA). To confirm that the observed responses were mediated by muscarinic receptors, some assays were carried out in the presence of atropine (10 µM). E<sub>max</sub> and EC<sub>50</sub> values were obtained from OXO-M and compound 16 concentration-response curves using GraphPad Prism 4.0 software.

#### ***Antagonism assay.***

To examine whether compounds 12, 13, and 20 were able to block M<sub>3</sub> receptor-mediated responses, we determined their ability to inhibit OXO-M-induced increases in intracellular calcium levels via activation of M<sub>3</sub> receptors endogenously expressed by MIN6 cells. 50,000 cells were seeded into 96-well plates and FLIPR assays were carried out as described above (Calcium Mobilization Assay). On the day of the assay, cells were pre-incubated with the calcium-chelating dye and the various compounds (atropine and compounds 12, 13, and 20) for 45 min, followed by the addition of the muscarinic receptor agonist OXO-M (1 μM). Compounds 12, 13, and 20 were used at a concentration of 10 μM (~10 times their K<sub>i</sub>). Atropine was employed at a concentration of 10 nM.

## Results

### ***Identification of new muscarinic ligands.***

To identify new muscarinic ligands and to assess the suitability of muscarinic receptor structures as templates for ligand discovery, we pursued a docking campaign against the M<sub>2</sub> muscarinic receptor structure. Like most GPCR structures available to date, the M<sub>2</sub> receptor was solved in an inactive conformation bound to a small molecule antagonist. It presents a deep, almost completely buried ligand binding site (Fig. 1A), covered by a layer of tyrosines long known to be critical for ligand binding. Such deeply buried cavities are well-suited to computational ligand discovery, and previous GPCR docking work has met with remarkable success (Sabio et al., 2008; Kolb et al., 2009; Katritch et al., 2010; Carlsson et al., 2010; de Graaf et al., 2011; Mysinger et al., 2012). Within the binding pocket, the crystallographic ligand quinuclidinyl benzilate (QNB) engages largely in hydrophobic interactions, while Asn404<sup>6.52</sup> forms a pair of hydrogen bonds and Asp103<sup>3.32</sup> serves as a counter ion to the positive charge of the ligand (Fig.

1B; superscript numerals refer to the Ballesteros-Weinstein numbering system for GPCRs).  
(Ballesteros and Weinstein, 1995)

We screened 3.1 million fragments or “lead-like” molecules (Methods) from the ZINC database (Irwin and Shoichet, 2005; Irwin et al., 2012) against the structure of the M<sub>2</sub> receptor. Each fragment and “lead-like” molecule was sampled in an average of 222 and 274 orientations and 437 and 700 conformations, respectively, in the orthosteric site; overall, over 547 billion configurations of the 3.1 million molecules were sampled. Molecules were ranked based on van der Waals and electrostatic complementarity, corrected for ligand desolvation using a receptor volume-based implementation of the Generalized-Born equation (Mysinger and Shoichet, 2010). From among the top 500 ranked molecules, we selected 18 that interacted with key residues such as Asp103<sup>3.32</sup>, Asn404<sup>6.52</sup>, and Trp400<sup>6.48</sup>, preferring molecules topologically or physically dissimilar to known muscarinic ligands. These 18 molecules were tested by single point competition binding against the high affinity antagonist <sup>3</sup>H-NMS (Supplementary table 1), and those with substantial inhibition at 20 μM were further tested in a competition binding assay. Of the 18 compounds tested, 11 had K<sub>i</sub> values lower than 50 μM (Table 1; Supplementary figure S1; Supplementary table 2). The compound with the highest affinity (Compound 1) displayed a K<sub>i</sub> of 390 nM. Six of these compounds were fragments, with ligand efficiencies (LEs) ranging from 0.36 to 0.44 kcal/heavy-atom. Most of the 11 molecules were topologically dissimilar to known muscarinic agents. Using two-dimensional ECFP4 fingerprints and Tanimoto coefficients (T<sub>c</sub>) (Hert et al., 2004) to all known muscarinic ligands in ChEMBL11 (Gaulton et al., 2011), 8 of the 11 compounds have a T<sub>c</sub> < 0.33 to the closest muscarinic ligand of any class, a difference large enough to be typically considered a “scaffold hop” (Muchmore et al., 2008). Correspondingly, their binding poses differ substantially from that of the co-crystallized ligand (Fig. 1C).

Intriguingly, two of the higher affinity ligands, compounds **5** and **11** (Table 1), lack the defining cationic amine that is ubiquitous among muscarinic ligands and other aminergic GPCRs (*e.g.*, histaminergic, adrenergic, dopaminergic, or serotonergic). Indeed, they were chosen for testing because of this unexpected physical property. Whereas in compound **5** the pyridine nitrogen might conceivably be cationic—though it would be expected to be neutral at physiological pH, and is docked in this form—compound **11** is constitutively neutral at all accessible pH values. Correspondingly, the phenyl analog of **5** and **11**, compound **12**, is also a ligand with low micromolar affinity. The loss of the Asp103<sup>3,32</sup> ion-pair with the ligand cation is a substantial insult, amounting to about 4 kcal/mol if one compares the affinity of compounds **11** and **12** to that of the analogous QNB, which binds with an affinity of 180 pM to the M<sub>2</sub> receptor (Heitz et al., 1999). However, the fact that such ligands can even bind to muscarinic receptors at meaningful reasonable concentrations has few precedents in the field (Barlow and Tubby, 1974). Indeed, No uncharged ligands of the M<sub>2</sub> or M<sub>3</sub> receptors are reported in the ChEMBL database (*i.e.*, all are expected to be ionized at physiological pH values), of the over 5000 ligands annotated, and while 4 neutral analogs of acetylcholine and other acetic-acid esters are reported to be active at acetylcholine receptors of the guinea-pig ileum (Barlow and Tubby, 1974), no further uncharged ligands have been reported subsequently, to the best of our knowledge.

### ***Docking for subtype selectivity.***

Though the docking against the M<sub>2</sub> receptor had no selectivity goal—compounds were simply chosen based on complementarity to the M<sub>2</sub> receptor—we were interested to learn whether the unusual chemotypes and physical properties of the new ligands conferred selectivity. We thus tested those M<sub>2</sub> ligands with K<sub>i</sub> values lower than 10 μM for binding to the M<sub>3</sub> receptor (Table 1; Supplementary figure S2) (those molecules with weaker affinity were not pursued). Intriguingly, all three uncharged ligands (**5**, **11**, and **12**) bear some selectivity for the M<sub>3</sub> over the M<sub>2</sub> subtype.

For example, compound **12** shows a 5-fold higher affinity for the M<sub>3</sub> subtype (K<sub>i</sub> = 290 nM) as compared to the M<sub>2</sub> subtype. Prompted by this observation, we explicitly set out to exploit the few differences that do exist between the M<sub>2</sub> and M<sub>3</sub> orthosteric sites in docking screens for subtype-selective ligands, treating the M<sub>2</sub> subtype as a docking 'anti-target'. In the M<sub>3</sub> receptor, M<sub>2</sub> Phe181 is replaced by a leucine, creating an enlarged pocket that might be exploited to achieve binding selectivity (Fig. 2A, B). We again docked the fragment and "lead-like" subsets of the ZINC database against both the M<sub>2</sub> and M<sub>3</sub> receptors, this time selecting the top-ranked 5,000 molecules against the M<sub>3</sub> receptor. From these compounds, we chose 500 molecules with the largest rank difference between subtypes (Fig. 2C; Table 2; Supplementary figure S3; Supplementary table 3). For instance, compound **13** ranks 2496 out of 3.1 million (top 0.1%) docked against the M<sub>3</sub> receptor, but ranks only 1,238,745 out of 3.1 million (top 40%) against the M<sub>2</sub> receptor, suggesting much better complementarity to the M<sub>3</sub> subtype. From these 500 molecules, 16 candidates were selected for testing, again weighing key interactions and chemical novelty (Table 2). Of these, 8 compounds showed detectable binding to the M<sub>3</sub> receptor. We then tested each of these molecules for affinity against both receptor subtypes. Although most compounds showed detectably higher affinity for the M<sub>3</sub> receptor, the selectivity ratios were typically modest, reaching at best 6-fold (Table 2). The one exception was compound **16**, a ligand with an unprecedented sulfonamide core and a ECFP4-based T<sub>c</sub> value of only 0.3 to the closest known muscarinic ligand in ChEMBL (Gaulton et al., 2011). This molecule proved to be a partial agonist at the M<sub>3</sub> receptor in a cell-based functional assay (5 μM EC<sub>50</sub> value) without detectable activity at the M<sub>2</sub> receptor (see below).

### ***Efficacy of new ligands.***

Most docking screens against inactive GPCR structures have discovered only antagonists (Kolb et al., 2009; Carlsson et al., 2010; Katritch et al., 2010; Carlsson et al., 2011; de Graaf et al., 2011), while a docking screening against the activated state of the β<sub>2</sub>-adrenergic receptor

discovered only agonists (Weiss et al., 2013). Thus far, the only exception to this pattern is the  $\kappa$  opioid receptor, where an inactive state was used as a template for the docking-based discovery of specific agonists (Negri et al., 2013). We therefore investigated the efficacy of the new ligands against both  $M_2$  and  $M_3$  receptors, using a calcium mobilization assay to test for G protein activation. The  $M_2$  receptor couples primarily to the  $G_i$  class of G proteins, which mediate inhibition of adenylyl cyclase, while the  $M_3$  receptor preferentially couples to  $G_{q/11}$ , mediating hydrolysis of phosphoinositide lipids and consequent elevation of intracellular calcium. For these assays, we used CHO cells stably expressing the human  $M_3$  receptor or CHO cells stably co-expressing the human  $M_2$  receptor and a hybrid G protein  $G_{q/11}$ , which comprises of a  $G\alpha_q$  subunit in which the last five amino acids were replaced with the corresponding  $G\alpha_i$  sequence, allowing coupling to the  $M_2$  receptor (Wess et al., 1997). Almost all compounds tested were devoid of agonist activity on either receptor. Additional functional studies with representative compounds showed that the uncharged compound **12** antagonized oxotremorine-M-induced activation of  $M_3$  receptors in cultured MIN6 cells, as did compounds **13** and **20** (Supplementary figure S4).

The only agent that showed agonist activity at the  $M_3$  receptor was compound **16**. This molecule was a partial agonist at the  $M_3$  receptor, with an  $EC_{50}$  of 5.2  $\mu$ M an  $E_{max}$  of 65%, but lacked detectable efficacy at the  $M_2$  subtype (Fig. 3). The lack of agonist activity of **16** at the  $M_2$  receptor was confirmed in both calcium mobilization (Fig. 3A) and adenylyl cyclase inhibition (Fig. 3B) assays. To our knowledge, compound **16** represents the first pharmacological agent that can activate  $M_3$  but not  $M_2$  receptors. This novel activity profile mirrors its unusual chemotype: unlike most muscarinic ligands, compound **16** cannot form a paired hydrogen bond with Asn<sup>6.52</sup>, as seen in the  $M_3$  cocrystal structure with tiotropium, and instead may hydrogen bond through its unique sulfonamide to Tyr<sup>3.33</sup> (Fig. 3C). Whether this configuration is

conserved in the activated  $M_3$  structure to which it must bind is uncertain at this time; we cannot now rule out the possibility that compound **16** may even bind in a completely unexpected manner, including even to allosteric pockets that may initiate activation in their own right (Bluml et al., 1994; Avlani et al., 2010; Gregory et al., 2010). Further studies will be required to definitively establish the binding site for compound **16**. For now, it is the novelty of this chemotype to which we attribute its unexpected activity and selectivity.

***Compound 16 stimulates insulin release in pancreatic  $\beta$ -cells.***

The  $M_3$  receptor is a critical regulator of acetylcholine-mediated glucose-dependent insulin release from pancreatic  $\beta$ -cells, and recent studies indicate that increasing  $M_3$  receptor signaling would be useful in the treatment of type 2 diabetes (Gautam et al., 2010; Ruiz de Azua et al., 2010). However, further study of this concept has been stymied by the lack of selective  $M_3$  agonists. We therefore tested the ability of compound **16**, a selective  $M_3$  agonist, to stimulate insulin release from pancreatic  $\beta$ -cells. Specifically, we incubated MIN6 insulinoma cells, a mouse  $\beta$ -cell line expressing endogenous  $M_3$  receptors, with increasing amounts of OXO-M, a potent muscarinic agonist, or compound **16**. Both compounds evoked a dose-dependent increase in insulin secretion, with a  $pEC_{50}$  of -4.21 and -5.75, respectively, for compound **16** and OXO-M. Compound **16** induced insulin secretion with an  $E_{max}$  58% that of OXO-M (Fig. 4). Insulin release could be blocked by 10  $\mu$ M atropine (Fig. 4B), confirming the involvement of  $M_3$  receptors.

## Discussion

Four major observations emerge from this study. First, docking to the M<sub>2</sub> and M<sub>3</sub> muscarinic receptors led to the identification of multiple compounds with new physical properties and new chemical scaffolds. Second, as observed for other GPCRs, the docking hit-rates were high, between 50 and 60% of the compounds tested were active, with lead-like molecules often having affinities in the 0.1 to 1 μM range and with fragments with ligand efficiencies often above 0.4 kcal/heavy-atom (de Graaf et al., 2011). Third, an effort to explicitly dock for molecules specific for the M<sub>3</sub> over the M<sub>2</sub> subtype largely failed to successfully exploit the admittedly small difference between the two orthosteric sites, likely reflecting weaknesses in our current rigid-receptor docking models. Fourth, whereas it is not clear that the discovery of compound **16** reflects on our ability to select against binding to the M<sub>2</sub> subtype—it may simply reflect the unexplored functionality of this compound—compound **16** represents an important novel pharmacologic tool in that it can activate M<sub>3</sub> but not M<sub>2</sub> receptors. These findings hint at the potential of a structure-based program to discover compounds with new chemistry and correspondingly new pharmacology.

A promise of structure-based discovery is the identification of molecules that physically complement a binding site but escape from trends emerging from classic structure-activity relationships. The muscarinic ligands are a good example of how a few key chemotypes and physical properties have come to dominate an area of pharmacology. Of over 5000 M<sub>2</sub> or M<sub>3</sub> receptor ligands annotated in ChEMBL, all bear at least a single cationic nitrogen. The discovery of ligands that are constitutively uncharged demonstrates that orthosteric site binding in muscarinic receptors is not contingent on the presence of such a cationic group. Since both cationic and uncharged ligands were found in our screen, and ranked about equally in the



docking screen, this discovery also attests to the ability of a physics-based docking scoring function to balance high-magnitude ionic interactions (favoring charged ligands) and desolvation (favoring uncharged ligands) to arrive at a list of uncharged and cationic candidates. The uncharged ligands may balance the loss of the energy contributed by the Asp<sup>3.32</sup> ion pair by hydrogen bonds with Asn<sup>6.52</sup> and quadrupolar stacking with Tyr<sup>6.51</sup> and Trp<sup>6.48</sup>, as observed in the docked poses (Fig. 1). These interactions are less common among cationic docking hits, which tend to be dominated by the Asp<sup>3.32</sup> interaction (Fig. 1). Whereas the uncharged ligands bind as well as the new cationic ligands discovered here, they do lose about 4.5 kcal/mol in affinity compared to a structurally similar cationic ligand like QNB, attesting to the importance of the ion-pair in contributing to high affinity ligand binding. Still, as uncharged ligands will typically exhibit much greater membrane permeability than charged counterparts, such agents may show unique properties *in vivo* and may merit further exploration.

While the promise of discovering ligands with new chemotypes and new physical properties was realized in the docking screens, that of targeting particular differences between the M<sub>2</sub> and M<sub>3</sub> receptors to identify subtype-selective ligands was not. Though docking found molecules that fit much better against the rigid M<sub>3</sub> than the M<sub>2</sub> receptor structure owing to clashes with the larger Phe181 of the M<sub>2</sub> site, these apparent structural specificities largely disappeared on pharmacologic testing. Despite much more favorable M<sub>3</sub> docking ranks and scores (Table 2), experimental preference for the M<sub>3</sub> subtype never rose above six-fold in binding affinity. Thus, the steric clashes with Phe181 in the M<sub>2</sub> site were not realized, or only to a small degree, presumably reflecting conformational flexibility in the site. This has largely been true of other recent efforts to find molecules selective among different GPCR subtypes: where selective molecules have been found directly from docking, they may reflect more on the chemical novelty of the compounds than on specific interactions captured by the modeling (de Graaf et al., 2011; Carlsson et al., 2011; Kolb et al., 2012). The exception to this is where chemical

synthesis of multiple analogs, guided by structure, has followed initial hit-discovery by virtual screening (Langmead et al., 2012). Whereas there are now several methods that allow one to model local receptor flexibility in docking (Durrant and McCammon, 2010; Henzler and Rarey, 2011), implementing these prospectively in a way that does not lead to the appearance or even dominance of non-binding decoys remains an ongoing challenge (Wei et al., 2004; Totrov and Abagyan, 2008). As the structures of more receptor subtypes are being solved or become amenable to homology modeling, the call for reliable methods that can exploit small differences in receptor structure among closely related subtypes will become increasingly pressing. Correspondingly, the call for strategies that exploit differences among allosteric sites, which are often substantially greater than those between the orthosteric sites of receptor subtypes (Conn et al., 2009a; May et al., 2007), is also supported by this study. In all such efforts, a close collaboration with medicinal chemistry will be crucial, as one cannot usually expect that just the right, specific molecule will be present even as large a library as ZINC represents, even though a lead chemotype might be.

Though we were unable to reliably exploit the subtle differences between the M<sub>2</sub> and M<sub>3</sub> orthosteric sites to identify M<sub>3</sub> selective antagonists, the discovery of a selective M<sub>3</sub> receptor agonist (compound **16**) hints at the promise of a structure-based discovery program. Whereas the unusual pharmacology of compound **16** may owe as much to its chemical novelty as to the differential docking, the exploration of new chemotypes is something that has been often realized in docking campaigns against GPCRs (Evers and Klebe, 2004; de Graaf et al., 2011; Langmead et al., 2012) and that can be relied on. The observation that this agent can induce insulin release from pancreatic b-cells in culture supports its status as a lead compound for chemical tool development, and this finding may have important therapeutic implications for the treatment of type 2 diabetes if selective M<sub>3</sub> receptor agonists endowed with higher affinity can be developed. More broadly, a structure-based program of ligand discovery against the M<sub>3</sub>

receptor and related GPCRs holds out the promise of identifying new chemotypes with new physical properties and correspondingly new specificities and pharmacological properties, with important implications for the discovery of new probes and therapeutic leads.

## **Acknowledgements**

We thank Corey Liu and Aashish Manglik for technical assistance with NMR spectroscopy. We thank Dr. Allan I. Levey (Emory University) for kindly providing the two stable CHO cell lines.

## **Authorship contributions**

*Participated in research design:* Kruse, Weiss, Wess, Kobilka, and Shoichet.

*Conducted experiments:* Kruse, Weiss, K. Hu, J. Hu, Rossi.

*Contributed new reagents or analytic tools:* Eitel, Gmeiner.

*Performed data analysis:* Kruse, Weiss, Wess, Kobilka, and Shoichet.

*Wrote or contributed to the writing of the manuscript:* Kruse, Weiss, Wess, Kobilka, and Shoichet.

## References

Avlani VA, Langmead CJ, Guida E, Wood MD, Tehan BG, Herdon HJ, Watson JM, Sexton PM and Christopoulos A (2010) Orthosteric and allosteric modes of interaction of novel selective agonists of the M1 muscarinic acetylcholine receptor. *Molecular pharmacology* **78**(1): 94-104.

Barlow RB and Tubby JH (1974) Actions of some esters of 3,3-dimethylbutan-1-ol (the carbon analogue of choline) on the guinea-pig ileum. *Br J Pharmacol* **51**: 95-100.

Ballesteros J and Weinstein H (1995) Integrated methods for modeling G-protein coupled receptors. *Methods Neurosci* **25**: 366-428.

Bluml K, Mutschler E and Wess J (1994) Functional role in ligand binding and receptor activation of an asparagine residue present in the sixth transmembrane domain of all muscarinic acetylcholine receptors. *The Journal of biological chemistry* **269**(29): 18870-18876.

Caccamo A, Fisher A and LaFerla FM (2009) M1 agonists as a potential disease-modifying therapy for Alzheimer's disease. *Curr Alzheimer Res* **6**(2): 112-117.

Carlsson J, Coleman RG, Setola V, Irwin JJ, Fan H, Schlessinger A, Sali A, Roth BL and Shoichet BK (2011) Ligand discovery from a dopamine D3 receptor homology model and crystal structure. *Nat Chem Biol* **7**(11): 769-778.

Carlsson J, Yoo L, Gao ZG, Irwin JJ, Shoichet BK and Jacobson KA (2010) Structure-based discovery of A2A adenosine receptor ligands. *J Med Chem* **53**(9): 3748-3755.

Chan WY, McKinzie DL, Bose S, Mitchell SN, Witkin JM, Thompson RC, Christopoulos A, Lazareno S, Birdsall NJM, Bymaster FP and Felder CC (2008) Allosteric modulation of the muscarinic M4 receptor as an approach to treating schizophrenia. *Proc Natl Acad Sci USA* **105**(31): 10978-10983.

Conn PJ, Christopoulos A and Lindsley CW (2009a) Allosteric modulators of GPCRs: a novel approach for the treatment of CNS disorders. *Nat Rev Drug Discov* **8**(1): 41-54.

Conn PJ, Jones CK and Lindsley CW (2009b) Subtype-selective allosteric modulators of muscarinic receptors for the treatment of CNS disorders. *Trends Pharmacol Sci* **30**(3): 148-155.

Costanzi S, Santhosh Kumar T, Balasubramanian R, Kendall Harden T and Jacobson KA (2012) Virtual screening leads to the discovery of novel non-nucleotide P2Y(1) receptor antagonists. *Bioorganic & medicinal chemistry* 20(17): 5254-5261.

de Graaf C, Kooistra AJ, Vischer HF, Katritch V, Kuijjer M, Shiroishi M, Iwata S, Shimamura T, Stevens RC, de Esch IJ and Leurs R (2011) Crystal structure-based virtual screening for fragment-like ligands of the human histamine H(1) receptor. *J Med Chem* 54(23): 8195-8206.

Durrant JD and McCammon JA (2010) Computer-aided drug-discovery techniques that account for receptor flexibility. *Current opinion in pharmacology* 10(6): 770-774.

Evers A and Klebe G (2004) Successful virtual screening for a submicromolar antagonist of the neurokinin-1 receptor based on a ligand-supported homology model. *J Med Chem* 47(22): 5381-5392.

Gaulton A, Bellis LJ, Bento AP, Chambers J, Davies M, Hersey A, Light Y, McGlinchey S, Michalovich D, Al-Lazikani B and Overington JP (2011) ChEMBL: a large-scale bioactivity database for drug discovery. *Nucleic Acids Res.*

Gautam D, Ruiz de Azua I, Li JH, Guettier JM, Heard T, Cui Y, Lu H, Jou W, Gavrilova O, Zawalich WS and Wess J (2010) Beneficial metabolic effects caused by persistent activation of beta-cell M3 muscarinic acetylcholine receptors in transgenic mice. *Endocrinology* 151(11): 5185-5194.

Gregory KJ, Hall NE, Tobin AB, Sexton PM and Christopoulos A (2010) Identification of orthosteric and allosteric site mutations in M2 muscarinic acetylcholine receptors that contribute to ligand-selective signaling bias. *The Journal of biological chemistry* 285(10): 7459-7474.

Haga K, Kruse AC, Asada H, Yurugi-Kobayashi T, Shiroishi M, Zhang C, Weis WI, Okada T, Kobilka BK, Haga T and Kobayashi T (2012) Structure of the human M2 muscarinic acetylcholine receptor bound to an antagonist. *Nature* 482(7386): 547-551.

Heitz F, Holzwarth JA, Gies JP, Pruss RM, Trumpp-Kallmeyer S, Hibert MF and Guenet C (1999) Site-directed mutagenesis of the putative human muscarinic M2 receptor binding site. *Eur J Pharmacol* 380(2-3): 183-195.

Henzler AM and Rarey M (2011) Protein Flexibility in Structure-Based Virtual Screening: From Models to Algorithms, in *Virtual Screening* pp 223-244, Wiley-VCH Verlag GmbH & Co. KGaA.

Hert J, Willett P, Wilton DJ, Acklin P, Azzaoui K, Jacoby E and Schuffenhauer A (2004) Comparison of topological descriptors for similarity-based virtual screening using multiple bioactive reference structures. *Org Biomol Chem* **2**(22): 3256-3266.

Irwin JJ and Shoichet BK (2005) ZINC-a free database of commercially available compounds for virtual screening. *J Chem Inf Model* **45**(1): 177-182.

Irwin JJ, Shoichet BK, Mysinger MM, Huang N, Colizzi F, Wassam P and Cao Y (2009) Automated docking screens: a feasibility study. *J Med Chem* **52**(18): 5712-5720.

Irwin JJ, Sterling T, Mysinger MM, Bolstad ES and Coleman RG (2012) ZINC: A Free Tool to Discover Chemistry for Biology. *J Chem Inf Model* **52**(7): 1757-1768

Ishihara H, Asano T, Tsukuda K, Katagiri H, Inukai K, Anai M, Kikuchi M, Yazaki Y, Miyazaki JI and Oka Y (1993) Pancreatic beta cell line MIN6 exhibits characteristics of glucose metabolism and glucose-stimulated insulin secretion similar to those of normal islets. *Diabetologia* **36**(11): 1139-1145.

Katritch V, Jaakola VP, Lane JR, Lin J, Ijzerman AP, Yeager M, Kufareva I, Stevens RC and Abagyan R (2010) Structure-based discovery of novel chemotypes for adenosine A(2A) receptor antagonists. *J Med Chem* **53**(4): 1799-1809.

Kolb P, Rosenbaum DM, Irwin JJ, Fung JJ, Kobilka BK and Shoichet BK (2009) Structure-based discovery of beta2-adrenergic receptor ligands. *Proc Natl Acad Sci USA* **106**(16): 6843-6848.

Kolb P, Phan K, Gao Z, Marko AC, Sali A, Jacobson KA (2012) Limits of ligand selectivity from docking to models: in silico screening for A(1) adenosine receptor antagonists. *PLoS ONE* **7**(11) doi:10.1371/journal.pone.0049910

Kruse AC, Hu J, Pan AC, Arlow DH, Rosenbaum DM, Rosemond E, Green HF, Liu T, Chae PS, Dror RO, Shaw DE, Weis WI, Wess J and Kobilka BK (2012) Structure and dynamics of the M3 muscarinic acetylcholine receptor. *Nature* **482**(7386): 552-556.

Lorber DM and Shoichet BK (2005) Hierarchical docking of databases of multiple ligand conformations. *Current topics in medicinal chemistry* 5(8): 739-749.

Langmead CJ, Andrews SP, Congreve M, Errey JC, Hurrell E, Marshall FH, Mason JS, Richardson CM, Robertson N, Zhukov A and Weir M (2012) Identification of novel adenosine A(2A) receptor antagonists by virtual screening. *J Med Chem* 55(5): 1904-1909.

Li B, Scarselli M, Knudsen CD, Kim S-K, Jacobson KA, McMillin SM and Wess J (2007) Rapid identification of functionally critical amino acids in a G protein-coupled receptor. *Nat Meth* 4(2): 169-174.

Marlo JE, Niswender CM, Days EL, Bridges TM, Xiang Y, Rodriguez AL, Shirey JK, Brady AE, Nalywajko T, Luo Q, Austin CA, Williams MB, Kim K, Williams R, Orton D, Brown HA, Lindsley CW, Weaver CD and Conn PJ (2009) Discovery and characterization of novel allosteric potentiators of M1 muscarinic receptors reveals multiple modes of activity. *Mol Pharmacol* 75(3): 577-588.

May LT, Leach K, Sexton PM and Christopoulos A (2007) Allosteric modulation of G protein-coupled receptors. *Annu Rev Pharmacol Toxicol* 47: 1-51.

McMillin SM, Heusel M, Liu T, Costanzi S and Wess Jr (2011) Structural Basis of M3 Muscarinic Receptor Dimer/Oligomer Formation. *J Biol Chem* 286(32): 28584-28598.

Messer W (2002) The utility of muscarinic agonists in the treatment of alzheimer's disease. *J Mol Neurosci* 19(1): 187-193.

Mohr K, Tränkle C, Kostenis E, Barocelli E, De Amici M and Holzgrabe U (2010) Rational design of dualsteric GPCR ligands: quests and promise. *Br J Pharmacol* 159(5): 997-1008.

Muchmore SW, Debe DA, Metz JT, Brown SP, Martin YC and Hajduk PJ (2008) Application of belief theory to similarity data fusion for use in analog searching and lead hopping. *Journal of chemical information and modeling* 48(5): 941-948.

Mysinger MM and Shoichet BK (2010) Rapid context-dependent ligand desolvation in molecular docking. *J Chem Inf Model* 50(9): 1561-1573.



Mysinger MM, Weiss DR, Ziarek JJ, Gravel S, Doak AK, Karpiak J, Heveker N, Shoichet BK and Volkman BF (2012) Structure-based ligand discovery for the protein-protein interface of chemokine receptor CXCR4. *Proc Natl Acad Sci USA* **109**(14): 5517-5522.

Negri A, Rives ML, Caspers MJ, Prisinzano TE, Javitch JA and Filizola M (2013) Discovery of a Novel Selective Kappa-Opioid Receptor Agonist Using Crystal Structure-Based Virtual Screening. *J Chem Inf Model.* **53**(3): 521–526

Ruiz de Azua I, Scarselli M, Rosemond E, Gautam D, Jou W, Gavrilova O, Ebert PJ, Levitt P and Wess J (2010) RGS4 is a negative regulator of insulin release from pancreatic  $\beta$ -cells in vitro and in vivo. *Proc Natl Acad Sci USA* **107**(17): 7999-8004.

Sabio M, Jones K and Topiol S (2008) Use of the X-ray structure of the beta2-adrenergic receptor for drug discovery. Part 2: Identification of active compounds. *Bioorg Med Chem Lett* **18**(20): 5391-5395.

Totrov M and Abagyan R (2008) Flexible ligand docking to multiple receptor conformations: a practical alternative. *Current opinion in structural biology* **18**(2): 178-184.

Wei BQ, Weaver LH, Ferrari AM, Matthews BW and Shoichet BK (2004) Testing a flexible-receptor docking algorithm in a model binding site. *J Mol Biol* **337**(5): 1161-1182.

Weiss DR, Ahn S, Sassano MF, Kleist A, Zhu X, Strachan R, Roth BL, Lefkowitz RJ and Shoichet BK (2013) Conformation guides molecular efficacy in docking screens of activated beta-2 adrenergic G protein coupled receptor. *ACS Chem Biol* **8**(15): 1018-26.

Wess J, Liu J, Blin N, Yun J, Lerche C and Kostenis E (1997) Structural basis of receptor/G protein coupling selectivity studied with muscarinic receptors as model systems. *Life Sci* **60**(13-14): 1007-1014.

Wess J, Eglen RM and Gautam D (2007) Muscarinic acetylcholine receptors: mutant mice provide new insights for drug development. *Nat Rev Drug Discov* **6**(9): 721-733.

## Footnotes

A.C.K. & D.R.W. contributed equally to this work and should be considered co-first authors. Collaborative work on this project was supported by a US National Institutes of Health (NIH) grant [P01 GM106990] and by the National Science Foundation (NSF) grant [CHE-1223785]. Also supported and by NIH grants [R01 GM71896] (to BKS) and [R01 NS028471] (to BKK), and by the Mathers Charitable Foundation (to BKK). DRW was supported by NIH grant [F32 GM093580] and ACK is funded by an NSF Graduate Research Fellowship. The work of M.R., J.H., K.H., and J.W was supported by the Intramural Research Program of the NIH, National Institute of Diabetes and Digestive and Kidney Diseases (NIDDK). P.G. and K.E. acknowledge support from Bavaria California Technology Center.

**Figure 1. Docking poses for selected M<sub>2</sub> muscarinic receptor hits.** (a) The overall structure of the M<sub>2</sub> receptor (Haga et al., 2012) with the orthosteric site outlined. (b) The chemical structure of the co-crystallized antagonist QNB, its crystallographic geometry and key interactions (dashed lines). (c). Docking-discovered ligands (carbons in cyan) are superimposed in their docked poses on the crystallographic structure of QNB (carbons in yellow).

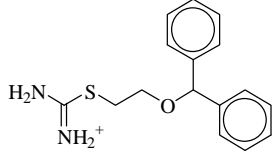
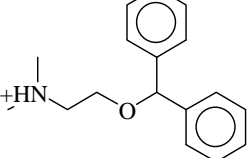
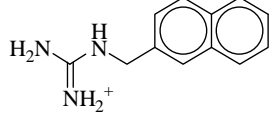
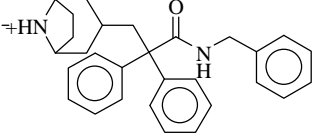
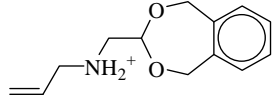
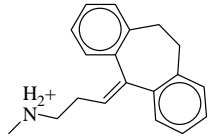
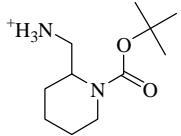
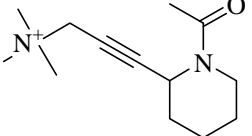
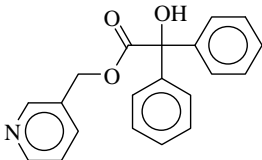
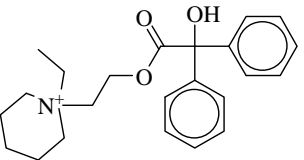
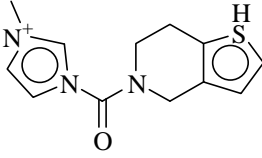
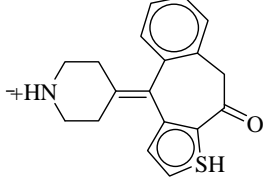
**Figure 2. Docking for selective M<sub>3</sub> receptor ligands.** (a) The M<sub>3</sub> (green) and M<sub>2</sub> receptor (orange) binding pockets are superimposed, and rendered as solvent-accessible surfaces, highlighting the enlarged binding pocket in the M<sub>3</sub> subtype (Kruse et al., 2012). (b) specific interactions with the co-crystallized M<sub>3</sub> antagonist tiotropium are shown. (c) Docking poses for select new ligands.

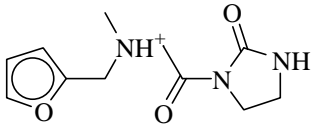
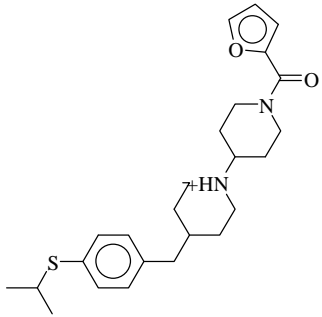
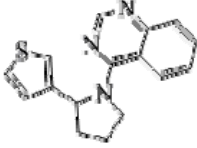
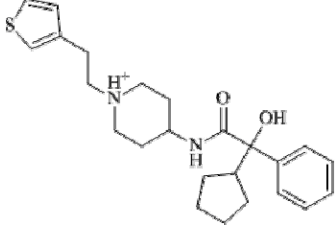
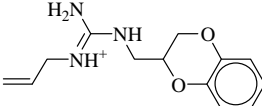
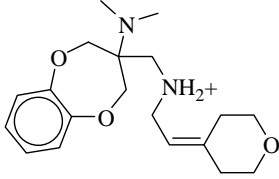
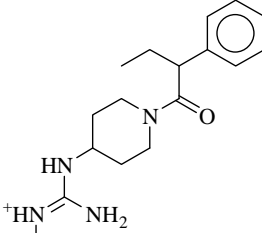
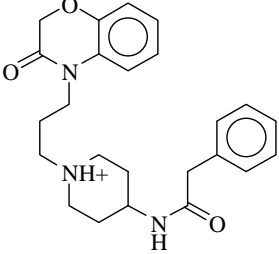
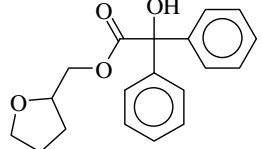
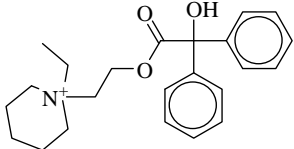
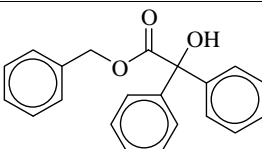
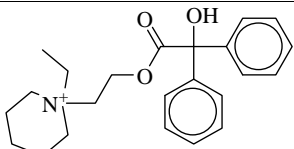
**Figure 3. Compound 16 activates M<sub>3</sub> but not M<sub>2</sub> receptors.** (a) Compound **16** showed partial agonism at the M<sub>3</sub> subtype, but not at the M<sub>2</sub> receptor in a calcium mobilization assay using CHO cells stably expressing M<sub>2</sub> or M<sub>3</sub> receptors (see Materials and Methods for details). This effect was blocked by the muscarinic antagonist atropine, consistent with direct activity at the M<sub>3</sub> receptor. (b) In a FRET-based cAMP assay (see Material and Methods for details), compound **16** did not lead to changes in intracellular cAMP levels in CHO-M<sub>2</sub> cells, confirming that this agent lacks efficacy at M<sub>2</sub> receptors. In this assay, an elevated 665 nm/620 nm ratio corresponds to decreased cAMP levels. The curves shown in panels (a) and (b) are representative of three independent experiments. (c) The unique structure and predicted binding mode of compound **16** may account for its novel activity profile.

**Figure 4. Ligand-stimulated insulin release in MIN6 cells.** (a) MIN6 cells, which express endogenous M<sub>3</sub> receptors, were incubated with increasing concentrations of OXO-M and

compound **16**, and ligand-induced insulin release was measured. (b) The responses to both agonists were sensitive to blockade by atropine, indicating that the observed effects result from direct M<sub>3</sub> receptor activation. Data (means ± SE) are from three independent experiments: OXO-M pEC<sub>50</sub> = 5.75 ± 0.17, E<sub>max</sub> = 453 ± 21; Compound **16** pEC<sub>50</sub> = 4.21 ± 0.18, E<sub>max</sub> = 261 ± 21.

**Table 1. Compounds identified by docking to M<sub>2</sub> receptor.**

Compound ID (ZINC ID) <sup>a</sup>	Structure	Docking Rank <sup>b</sup>	M <sub>2</sub> K <sub>i</sub> ± SEM <sup>c</sup>	M <sub>3</sub> K <sub>i</sub> ± SEM	Tc <sup>d</sup>	Closest analog <sup>e</sup>
1 (C30009023)		241 <sup>f</sup>	390 ± 32 nM	130 ± 3 nM	0.47	
2 (C01571130)		337 <sup>g</sup>	17 ± 2 μM	N.D. <sup>h</sup>	0.25	
3 (C02293082)		379 <sup>g</sup>	38 ± 6 μM	N.D.	0.23	
4 (C04202452)		89 <sup>g</sup>	39 ± 3 μM	N.D.	0.30	
5 (C13283175)		198 <sup>f</sup>	1.2 ± 0.2 μM	360 ± 65 nM	0.42	
6 (C32628700)		100 <sup>g</sup>	33 ± 8 μM	N.D.	0.23	

7 (C32810363)		299 <sup>g</sup>	21 ± 5 μM	N.D.	0.24	
8 (C48231657)		58 <sup>f</sup>	6.6 ± 1.4 μM	1.8 ± 1.3 μM	0.26	
9 (C58162941)		186 <sup>g</sup>	22 ± 4 μM	N.D.	0.24	
10 (C58406123)		46 <sup>f</sup>	4.7 ± 0.8 μM	5.8 ± 0.5 μM	0.32	
11 (C58857984)		370 <sup>f</sup>	2.0 ± 0.1 μM	1.2 ± 0.4 μM	0.46	
12 (C04547851)		Analog of Cmpd. 5	1.6 ± 0.1 μM	290 ± 48 nM	0.49	

<sup>a</sup>From <http://zinc.docking.org>

<sup>b</sup>Out of 3.1 million fragments and “lead-like” molecules docked to the M<sup>2</sup> receptor.

<sup>c</sup>Values are from a minimum of two independent measurements performed in triplicate

<sup>d</sup>ECFP4-based Tanimoto coefficient to the most similar muscarinic ligand in ChEMBL.

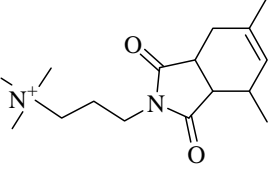
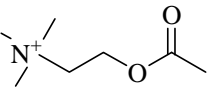
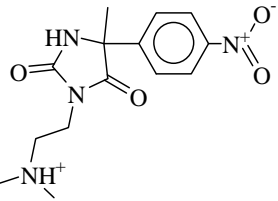
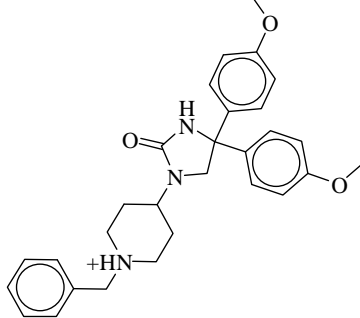
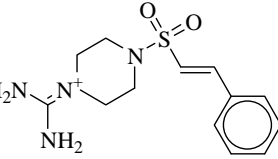
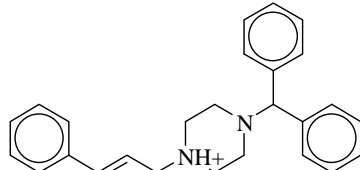
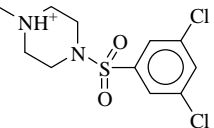
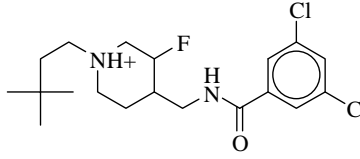
<sup>e</sup>Most similar molecule in ChEMBL.

<sup>f</sup>Rank among to 2662342 lead-like compounds

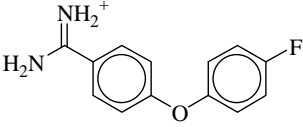
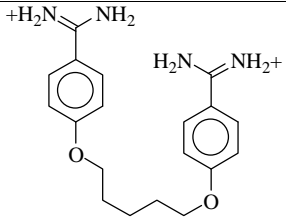
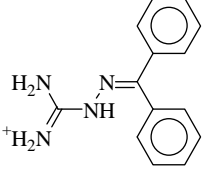
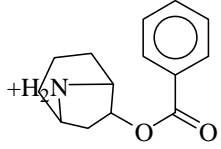
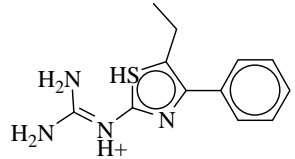
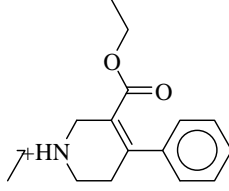
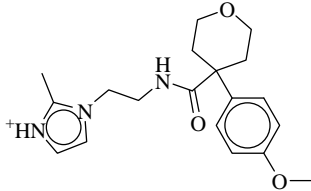
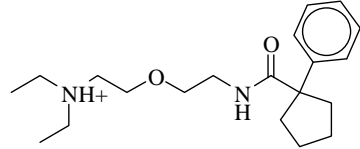
<sup>g</sup>Rank among 357594 fragments

<sup>h</sup>N.D. Not determined.

**Table 2. Compounds docking well to M<sub>3</sub> receptor and poorly to M<sub>2</sub> receptor.**

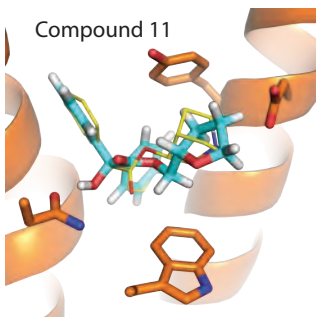
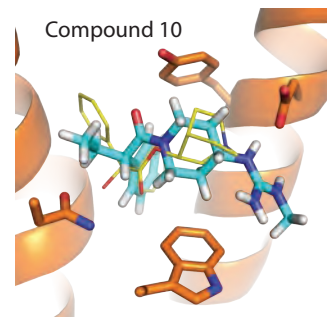
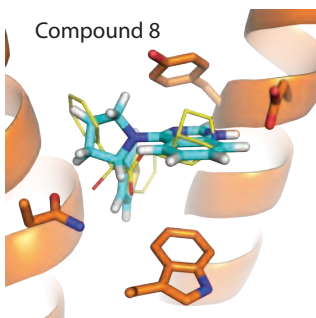
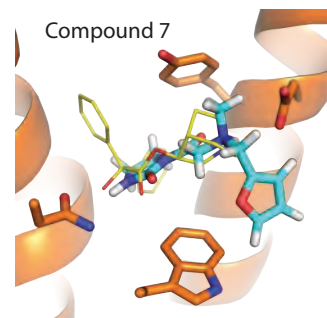
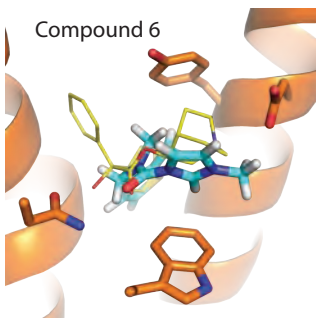
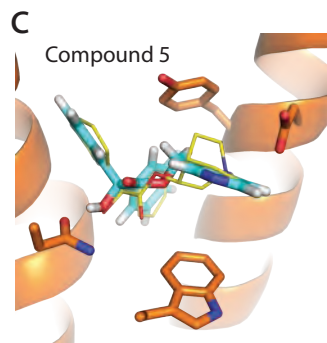
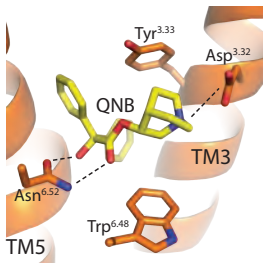
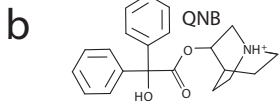
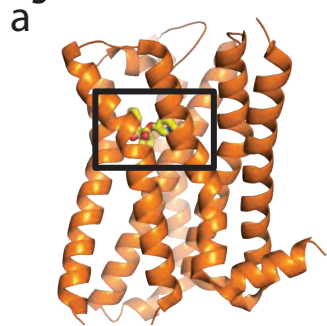
Compound ID (ZINC ID)	Structure	M <sub>2</sub> K <sub>i</sub> ± SEM <sup>a</sup> μM	M <sub>3</sub> K <sub>i</sub> ± SEM <sup>a</sup> μM	M <sub>3</sub> /M <sub>2</sub>	M <sub>3</sub> rank/ M <sub>2</sub> rank	T <sub>c</sub>	Closest analog
13 (C18061786)		8.2 ± 0.8 μM	1.3 ± 0.1 μM	6.3 fold	2496 / 1238745	0.21	
14 (C00181425)		16 ± 1.6 μM	10 ± 2.9 μM	1.1 fold	3278 / 1018801	0.24	
15 (C06850766)		89 ± 7.7 μM	64 ± 14 μM	1.4 fold	3728 / 1157022	0.29	
16 (C21270353)		>100 μM	>100 μM (K <sub>i</sub> )	N/A	4528 / 984037	0.30	



17 (C19866069)		24 ± 2.7 μM	5.1 ± 0.7 μM	4.8 fold	828/ 67487	0.48	
18 (C01694229)		18 ± 1.8 μM	8.8 ± 1.3 μM	2.0 fold	294 / 14466	0.23	
19 (C48433680)		740 ± 37 nM	780 ± 390 nM	1.0 fold	14 / 722	0.25	
20 (C49524426)		1.9 ± 0.5 μM	1.4 ± 0.4 μM	1.4 fold	369 / 471031	0.33	

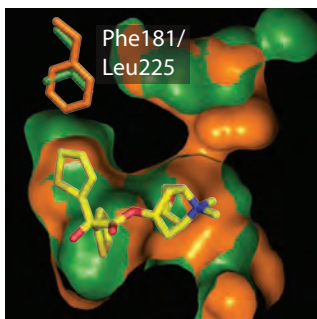
<sup>a</sup>Values are from a minimum of two independent measurements performed in triplicate

<sup>b</sup>EC<sub>50</sub> in a cell-based agonism assay (see Methods and Materials).

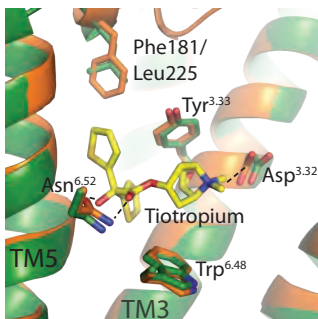
**Figure 1**

# Figure 2

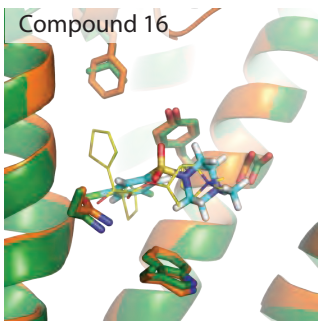
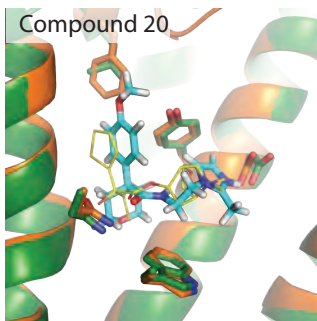
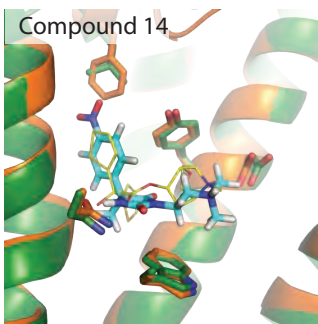
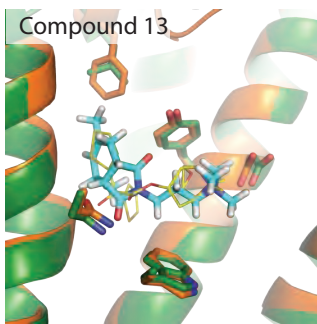
## A

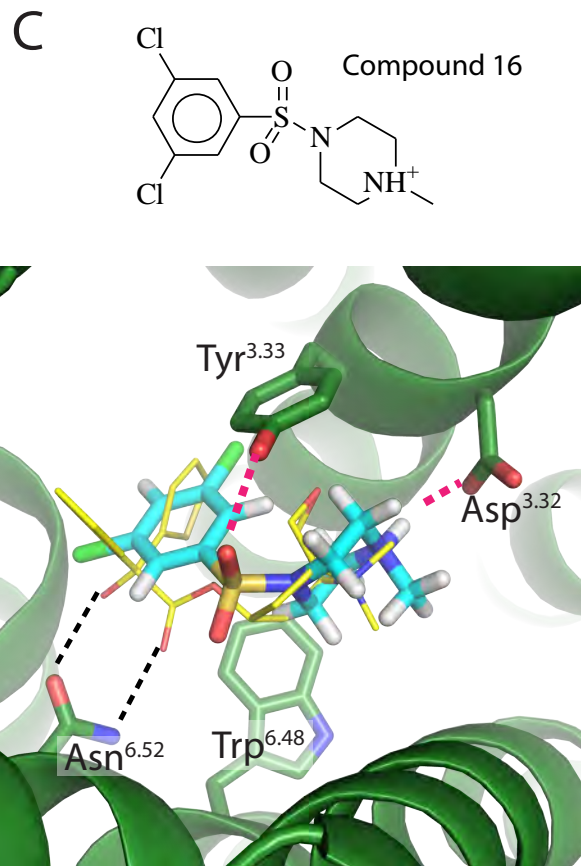
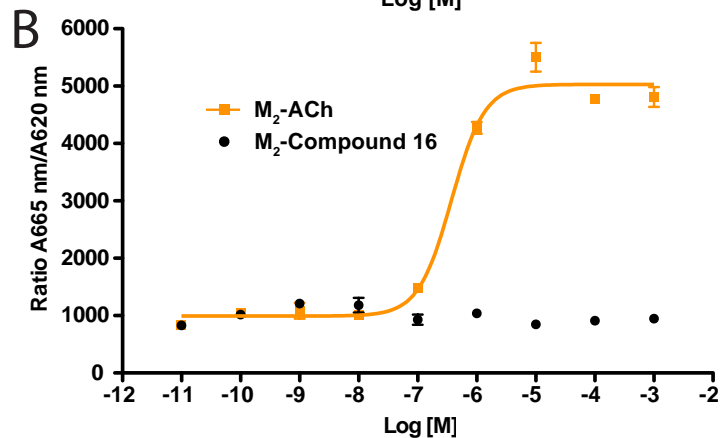
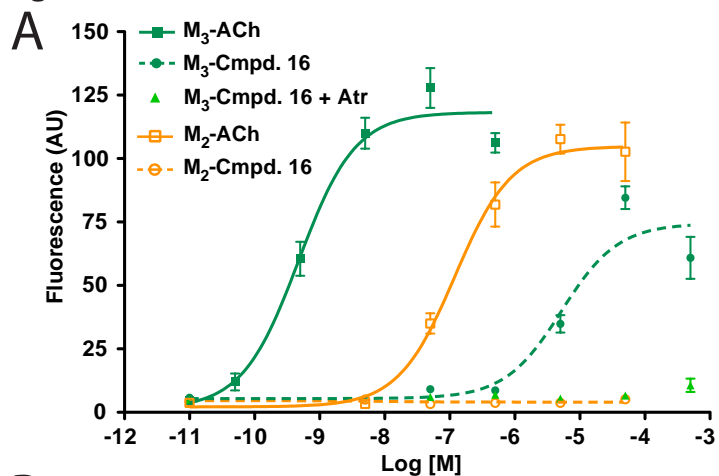


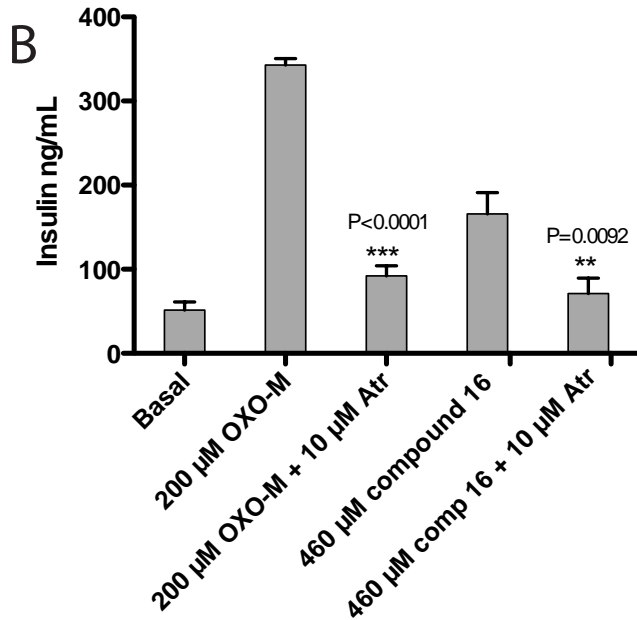
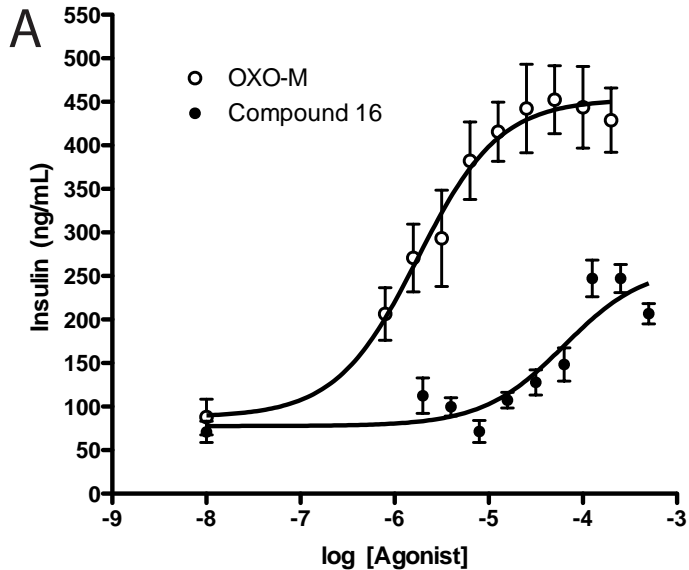
## B



## C



**Figure 3**

**Figure 4**

**Muscarinic receptors as model targets and antitargets  
for structure-based ligand discovery**

Andrew C. Kruse, Dahlia R. Weiss, Mario Rossi, Jianxin Hu, Kelly Hu, Katrin Eitel, Peter  
Gmeiner, Jürgen Wess, Brian K. Kobilka & Brian K. Shoichet

**Supplementary Information**

**Supplementary table 1. Ligand binding parameters for muscarinic receptors expressed in Sf9 cells.**

<b>Ligand</b>	<b>M<sub>2</sub> K<sub>i</sub></b>	<b>M<sub>3</sub> K<sub>i</sub></b>	<b>M<sub>2</sub> K<sub>d</sub></b>	<b>M<sub>3</sub> K<sub>d</sub></b>
<sup>3</sup> H N-methyl scopolamine	–	–	390 ± 30 pM	210 ± 32 pM
Atropine	890 ± 33 pM	760 ± 54 pM	–	–
Carbachol	33 ± 3.4 μM	120 ± 13 μM	–	–

Measurements in each case are mean ± SEM of at least two independent experiments performed in triplicate.

**Supplementary table 2. Compounds tested that did not bind the muscarinic M<sub>2</sub> receptor.**

<b>Non-binders to M<sub>2</sub> receptor (ZINCID):</b>
C04992661
C05059535
C19864940
C32912674
C43653471
C04808018
C29334436
C04992661

**Supplementary table 3. Compounds tested that did not bind the muscarinic M<sub>3</sub> receptor.**

<b>Non-binders to M<sub>3</sub> receptor (ZINCID):</b>
C19424506
C12554628
C55392956
C03378303
C06184630
C13002737
C58125605
C63834631

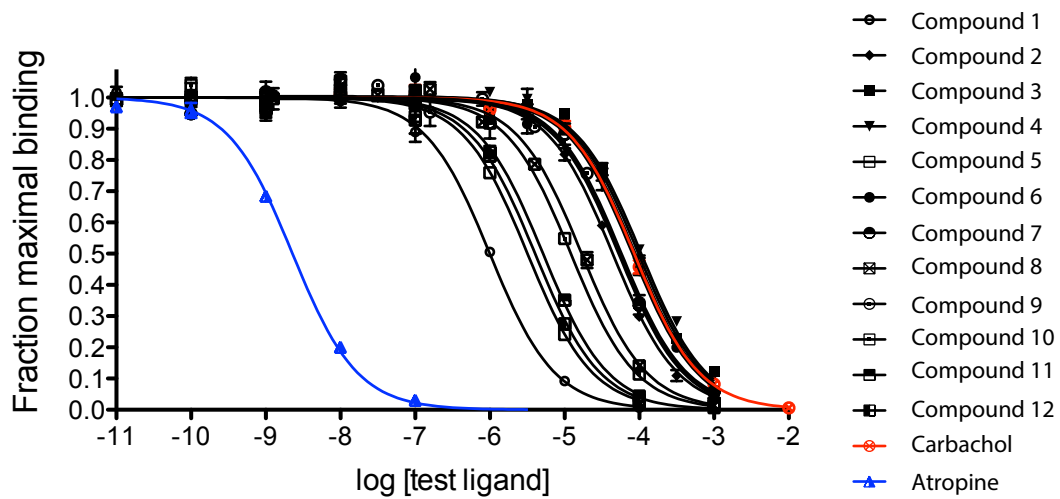


**Figure S1. <sup>3</sup>H NMS Competition curves for M<sub>2</sub> ligands.** Competition curves for M<sub>2</sub> docking hits binding to the M<sub>2</sub> receptor. Data points are shown as the mean +/- SEM of three measurements. The prototypical muscarinic agonist carbachol and the prototypical antagonist atropine are included for comparison.



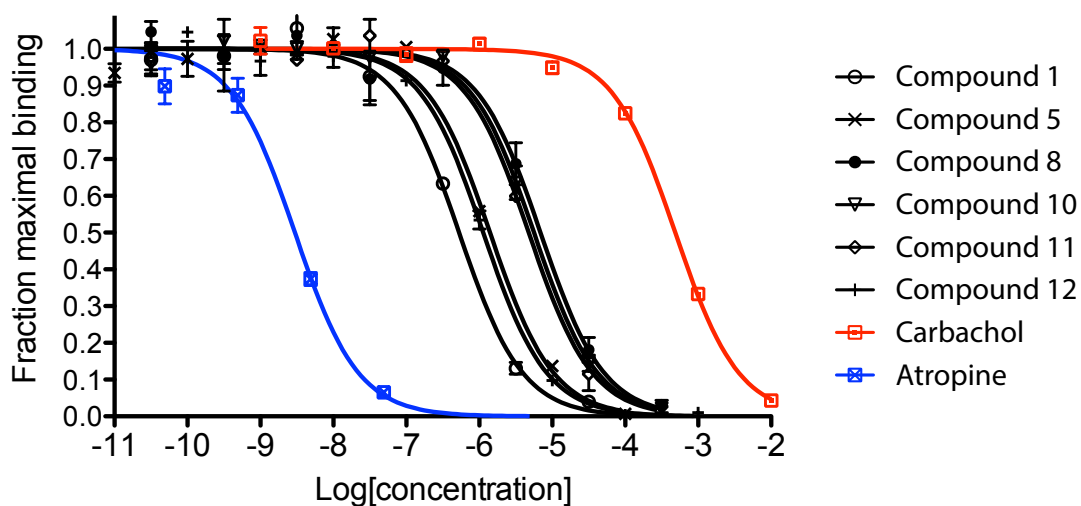


**Figure S2. <sup>3</sup>H NMS Competition curves for novel M<sub>2</sub> ligands binding to the M<sub>3</sub> receptor.** Competition curves for select M<sub>2</sub> docking hits binding to the M<sub>2</sub> receptor. All compounds with affinities greater than 10 μM for the M<sub>2</sub> receptor were tested for binding to M<sub>3</sub>. Data points are shown as the mean +/- SEM of three measurements. The prototypical muscarinic agonist carbachol and the prototypical antagonist atropine are included for comparison.

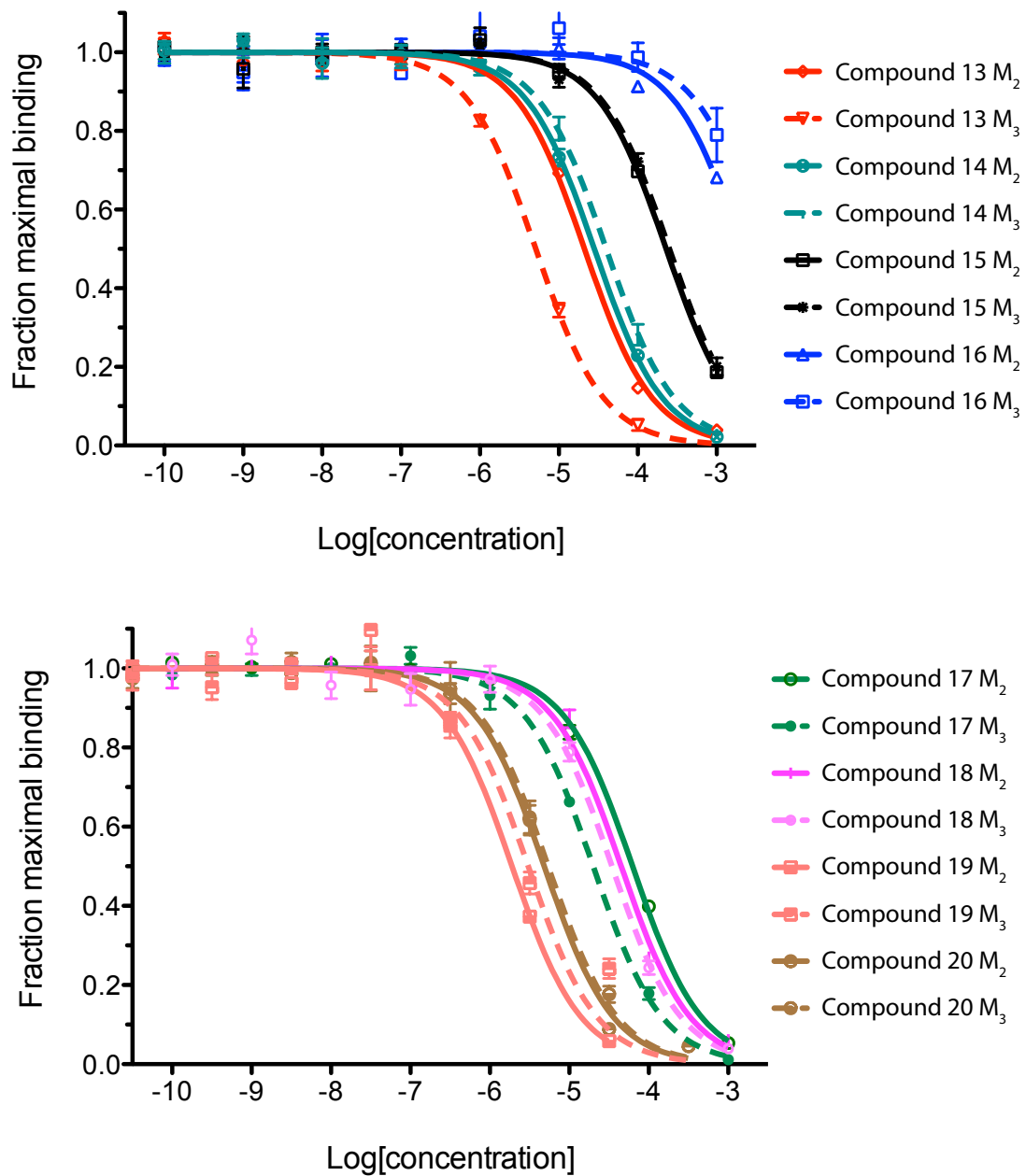


**Figure S3. <sup>3</sup>H NMS Competition curves for M<sub>3</sub> ligands.** Competition curves for M<sub>3</sub> docking hits binding to the M<sub>2</sub> (solid lines) and M<sub>3</sub> receptors (dotted lines). Data points are shown as the mean +/- SEM of three measurements.

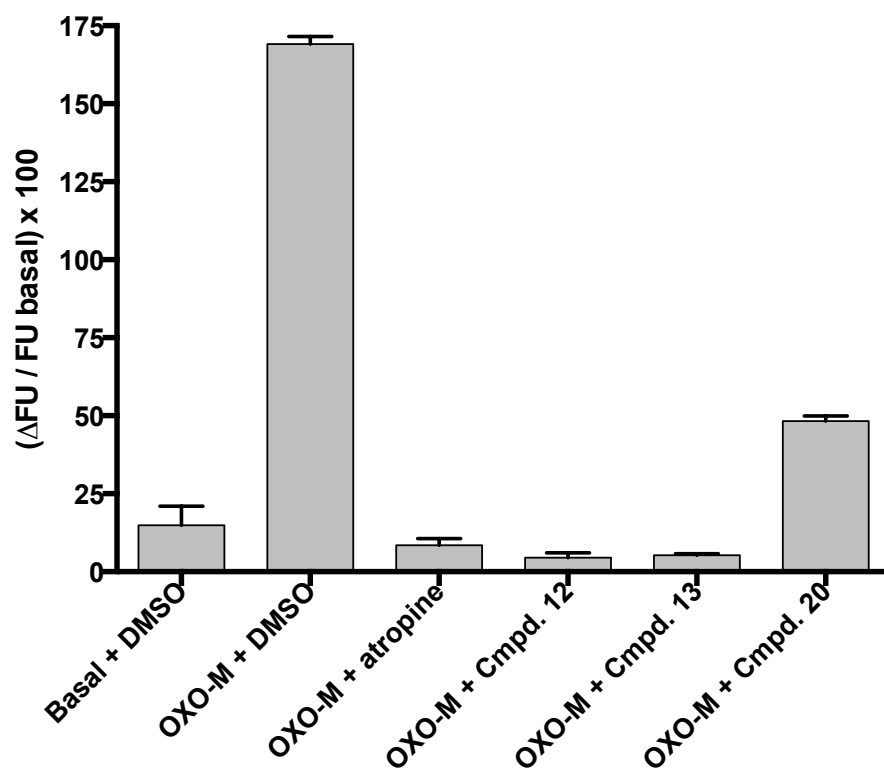


**Figure S4. Functional antagonism of selected ligands.** Three representative compounds were chosen for direct measurement of antagonist activity: compounds 12, 13, and 20. Each of these agents was able to block or severely impair activation of endogenous  $M_3$  receptors in MIN6 cells by the agonist OXO-M (readout: OXO-M-induced increases in intracellular calcium levels). The following drug concentrations were used: OXO-M, 1  $\mu$ M; compounds 12, 13, and 20: 10  $\mu$ M ( $\sim$ 10 times their  $K_i$ ); atropine, 10 nM. Data represent means  $\pm$  SEM from two independent experiments. Assays were performed in six repeats.